JOURNAL OF CATALYSIS 149, 364–374 (1994)

Manganese Oxides as Catalysts for the Selective Reduction of Nitrobenzene to Nitrosobenzene

Annemarieke Maltha, Thomas L. F. Favre, Heleen F. Kist, Adrianus P. Zuur, and Vladimir Ponec[1]

Gorlaeus Laboratories, Leiden University, P.O. Box 9502, 2300 RA Leiden, The Netherlands

Received December 20, 1993; revised June 24, 1994

The activity and selectivity of various MnO_x catalysts for the selective reduction of nitrobenzene to nitrosobenzene have been studied, measuring the rate in a continuous flow reactor. Characterisation of the catalysts has been performed with XRD, IR, UV/VIS, EM, and TPR. It appeared that the steady-state catalyst is in all cases the spinel Mn_3O_4 in a slightly reduced form. Without the addition of an external reductant to the feed, nitrobenzene was not only reduced but also oxidised, which created oxygen vacancies in the catalyst surface. Addition of an external reductant did not cause a change in the amount of nitrosobenzene formed, but the concentration of side products, like aniline and dimerisation products, increased. It is suggested that the selective reduction of nitrobenzene with the catalyst Mn_3O_4 runs by the Mars and Van Krevelen mechanism.

INTRODUCTION

In industrial organic chemistry, it is often very desirable to insert an oxygen atom into an organic molecule (selective oxidation) or to remove it (selective reduction) from a molecule having more than one oxygen atom. The first reactions mentioned have already been studied extensively with metal oxides as catalysts. It has been established that these reactions have, in almost all cases, a form of the so-called Mars and Van Krevelen mechanism (1). In this mechanism, a molecule is oxidised by lattice oxygen and, subsequently, the oxygen vacancy is replenished by dioxygen from the reaction mixture. An attractive possibility is to use the reoxidation step of the catalyst for a selective reduction reaction, like that of nitrobenzene to nitrosobenzene.

The selective reduction of nitrobenzene to nitrosobenzene not only is a very suitable model for studying the fundamental problems of selective reductions, but also has some commercial potential (2, 3). Nitrosobenzene is used as an intermediate in organic syntheses and in the production of antioxidants for various applications. In the past it was produced by a two-step reaction: reduction of nitrobenzene to phenylhydroxylamine using Zn and HCl and then oxidation to nitrosobenzene using chromates. However, a one-step gas phase reduction is much more preferable, because this reaction produces fewer waste products. Patents (2, 3) recommend, for example, manganese oxide promoted by sodium compounds as a suitable catalyst for the gas phase reduction reaction.

Our exploratory research (4) revealed that MnO_2 was initially inactive in the selective reduction of nitrobenzene. However, the steady state of the catalyst can differ very much from the initial state of the oxide by which the reactor has been filled (5) and lower oxides appeared to be active.

METHODS

Catalyst Preparation

The catalysts of the nominal composition MnO, α-Mn_3O_4, α-Mn_2O_3, and β-MnO_2 were synthesised as follows: MnO was prepared by the gas phase reduction of α-Mn_3O_4 using a 5% H_2/N_2 gas mixture at 973 K, for 20 h.

Three different preparations of α-Mn_3O_4 were used in this study:

a. A solution of NH_4OH was added to a solution of $Mn(NO_3)_2$ until pH 9 was reached, whereafter the hydroxide was dried at 400 K in air and heated at 673 K under a flow of N_2 for 2 h to produce Mn_3O_4 labelled (a). Mn_3O_4 prepared in essentially the same way but dried at 410 K will be called Mn_3O_4(ox).

b. A solution of $Mn(NO_3)_2$ was added dropwise to a solution of NH_4OH, keeping a constant pH of 9.6 (Mn_3O_4(b)). The precipitate was dried in air at 350 K.

c. β-MnO_2 was reduced using a flow of pure H_2 at 573 K for 2 h (Mn_3O_4(c)).

α-Mn_2O_3 was synthesised by oxidation of Mn_3O_4(a) for 1.5 h in a flow of pure O_2 at 573 K. β-MnO_2 (pyrolusite) was prepared by the thermal decomposition of $Mn(NO_3)_2$ in air, at 400 K.

[1] To whom correspondence should be addressed.

0021-9517/94 $6.00

TABLE 1

Colour and Lattice Constants of Various Manganese Oxides before and after the Reaction with Nitrobenzene

Catalyst[a]	Colour before reaction	Colour after reaction	Lattice constant before reaction (nm)	Lattice constant after reaction (nm)
MnO	Green	Brown	—	0.5764, 0.9418 (Mn_3O_4)
Mn_3O_4(a)	Brown	Brown	0.5767, 0.9475	0.5765, 0.9469
Mn_2O_3	Black	Black	0.9439	0.9412 (Mn_2O_3)
			—	0.5759, 0.9460 (Mn_3O_4)
β-MnO_2	Black	Brown	0.4405, 0.2876	—
			—	0.58322, 0.96137 (Mn_3O_4)

[a] In the initial state.

Catalytic Data: Measurements and Evaluation

Activity and selectivity measurements were carried out in an open flow system with a fixed bed reactor. The standard temperature of the reaction was 573 K, the carrier gas was helium, the nitrobenzene pressure of 70 Pa (total pressure was 1 bar) was achieved in a saturator, and the flow rate was 25 ml/min. Analysis was performed on-line by a GC, using an automatically driven sampling valve.

Nonvolatile products, which sometimes appeared in the "cold" parts of the apparatus, were analysed by a UV/VIS spectrometer. The reaction was carried out either without an external reductant (autoredox reaction) or with an external reductant (H_2, CH_4, CO).

Catalyst Characterisation

Catalysts were analysed by X-ray powder diffraction (XRD) and the total surface area measurements were performed with a Quantasorb apparatus of Quantachrome. Thermal programmed reduction (TPR) experiments were carried out using a gas flow of 67% H_2/Ar with a flow rate of 8.8 μmol H_2/s.

Furthermore, in some cases the catalysts were analysed by UV/VIS spectroscopy and IR spectroscopy. Elemental analysis was performed with Mn_3O_4, by means of a redox titration.

RESULTS

Characterisation of the Catalysts: XRD, UV/VIS, IR, and Surface Area Measurements

X-ray powder diffraction confirmed that, indeed, the compounds MnO, α-Mn_3O_4, α-Mn_2O_3, and β-MnO_2 were synthesised without any other compound detectable by XRD. Moreover, the various manganese oxides have the "right" colour: green for MnO, brown for Mn_3O_4, black for Mn_2O_3, and black for MnO_2, as shown in Table 1. When Mn_3O_4 contains nonstoichiometric oxygen as with Mn_3O_4(ox), the colour becomes dark brown. However, this preoxidised Mn_3O_4 shows the same diffraction pattern and nearly the same UV/VIS spectrum as Mn_3O_4. This was also observed by Bricker (6), who reported that the brown colour of Mn_3O_4 becomes darker during mild oxidation, while the oxidation state of the oxide increases from $MnO_{1.33}$ to $MnO_{1.44}$. Bricker suggested that during the oxidation of Mn_3O_4, γ-Mn_2O_3 was formed, of which the XRD pattern cannot be distinguished from that of Mn_3O_4. It is also possible that a thin layer of another Mn_2O_3, not detectable by XRD, was formed on the surface of Mn_3O_4. From IR experiments, no difference can be seen between Mn_3O_4(a) and Mn_3O_4(ox).

With the "MnO" catalyst, the XRD pattern shows after a 24-h reaction with nitrobenzene that an additional phase of Mn_3O_4 (broad peaks of Mn_3O_4, sharp peaks of MnO) was formed from MnO. Prolonging the time on stream to 72 h did not bring about any further change in the XRD pattern. The lattice constants of the Mn_3O_4 formed are slightly smaller than those of Mn_3O_4(a).

The X-ray diffractograms of the Mn_3O_4(a) catalyst do not show any difference when taken before and after the reaction. Mn_3O_4(a) has a tetragonal structure, with lattice constants of 0.5767 (a, b) and 0.9475 nm (c) before reaction and 0.5765 and 0.9469 nm after reaction. The XRD pattern of the catalyst that was Mn_2O_3 in the initial state also shows an additional phase of Mn_3O_4 after reaction. The lattice constants of this Mn_3O_4 are about equal to the lattice constants of Mn_3O_4(a).

MnO_2 has partially been converted into Mn_2O_3 and Mn_3O_4, after 24 h of reaction. After 72 h on stream the catalysts contain almost solely Mn_3O_4. The lattice constants of this Mn_3O_4 are somewhat larger than those of Mn_3O_4(a) (12).

UV/VIS experiments indicate that the catalysts Mn_3O_4 and Mn_2O_3 do not differ before and after the reaction, whereas, as seen by this technique, MnO changes into Mn_3O_4. The UV/VIS spectra of MnO_2 also show a change before and after the reaction with nitrobenzene, a change corresponding to the formation of Mn_3O_4.

Chemical analysis of Mn_3O_4(a) gives a mole ratio Mn^{3+}/Mn^{2+} of 2.18 before and a mole ratio of 1.90 after the reaction. The theoretical value for an ideal spinel is 2.00. The IR spectrum of fresh β-MnO_2 (pyrolusite) shows absorption bands at 663 (vs), 618 (vs), 405 (s), and 338 (ms) cm^{-1}. This spectrum corresponds well with data published by Potter and Rossman (7). The IR spectrum of the spent MnO_2 catalyst has absorption bands at 611 (vs), 498 (vs), 411 (m), and 343 (m) cm^{-1}.

The IR spectrum of freshly prepared Mn_3O_4 shows absorption bands at 633 (vs), 519 (vs), 413 (m), and 345 (m) cm^{-1}. The absorption bands between 650 and 500 cm^{-1} can be associated with coupled Mn–O stretching modes related to the tetrahedral and octahedral sites and the bands between 450 and 300 cm^{-1} with bond stretching modes of the octahedral sites with only a very small contribution of the tetrahedral sites (8). When the positions of the absorption bands are compared with those reported by Ishii *et al.* (8) for Mn_3O_4 prepared at 1573 K (612, 502, 412, and 352 cm^{-1}), a shift of about 20 cm^{-1} is observed for the two absorption bands with a considerable contribution of the stretching modes of the tetrahedral sites. This can be explained by the different temperatures used in the synthesis of Mn_3O_4: Ishii's sample was prepared at a much higher temperature than the catalyst studied here. Therefore, Ishii's sample is likely a stoichiometric Mn_3O_4, while our fresh catalyst prepared in air at lower temperatures is probably a nonstoichiometric manganese oxide of a formula Mn_3O_{4+x}. In the nonstoichiometric Mn_3O_{4+x} catalyst, some of the tetrahedral Mn^{2+} ions are oxidised to Mn^{3+} ions, which probably causes the absorption bands having a considerable contribution from the tetrahedral sites to be shifted to higher wavenumbers by about 20 cm^{-1}. The IR spectrum of the spent Mn_3O_4 catalyst shows absorption bands at 613 (vs), 498 (vs), 409 (m), and 342 (m) cm^{-1}. This spectrum is very similar to that of the spent "MnO_2" catalyst. The shift of the two absorption modes with a significant distribution of the tetrahedral sites is removed by the catalytic reaction with nitrobenzene. This result points to the following reaction scheme:

1. During the induction period the excess of oxygen in the non-stoichiometric Mn_3O_{4+x} is removed from the catalyst by (nonselective) oxidation of nitrobenzene (oxidation of the phenyl ring).
2. The steady state of the catalyst under the standard reaction conditions is very near that of a stoichiometric Mn_3O_4.

Morphology of the Mn_3O_4 Particles

A preliminary morphological analysis of some oxides was performed by transmission electron microscopy. In Methods, three different methods of Mn_3O_4 preparation were described. Observation by TEM shows that there is no difference in particle size distribution and in particle shapes between Mn_3O_4(a) and Mn_3O_4(b). The particle size distribution is very broad, from 1 to 100 nm. Some cubic-formed particles can be seen, but many particles have an irregular, not well-defined form. With a given catalyst, there is no visible difference in particle sizes and particle shapes before and after the catalytic reaction with nitrobenzene. However, Mn_3O_4, made from MnO_2 (Mn_3O_4(c)), shows a more regular picture: most of the particles have a tetragonally distorted cubic form and their size is about 25 to 40 nm. The latter observation is in a good agreement with the predictions made according to the Ziolkowski theory (9, 10). We shall turn to this point in another paper.

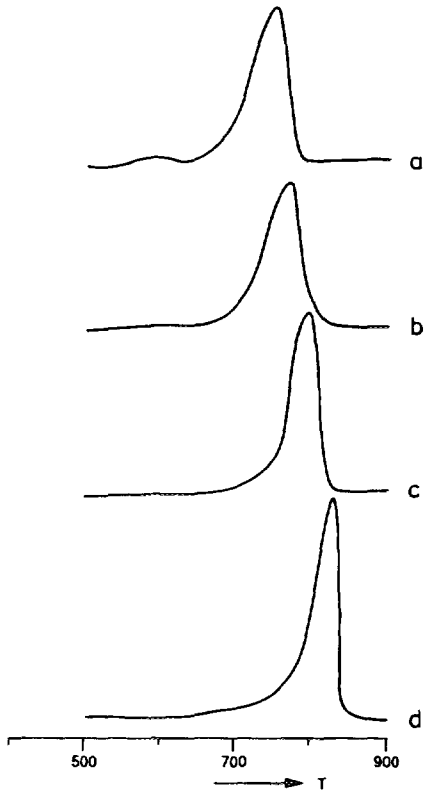

FIG. 1. TPR spectra of (a) fresh Mn_3O_4(a), (b) Mn_3O_4 after flushing with argon, (c) spent Mn_3O_4(a), and (d) Mn_3O_4(c).

Thermal Programmed Reduction

Figures 1a, 1b, 1c, and 1d show the TPR profiles of respectively (i) fresh $MnO_{1.33}$(a) (Mn_3O_4 is equal to $MnO_{1.33}$), (ii) Mn_3O_4(a) flushed with argon for 10 h at 573 K, (iii) spent Mn_3O_4(a), and (iv) fresh Mn_3O_4(c).

The measured O/Mn ratio of a fresh $MnO_{1.33}$(a) catalyst at 300 K is equal to 1.35, if we take the O/Mn ratio as being 1 after a complete reduction to MnO. Mn_3O_4(a) is reduced to MnO at 683 K. However, there is also an extra (small) peak at 483 K. When $MnO_{1.33}$ is first flushed with

TABLE 2

Rate of Reaction, Selectivity, Surface Area, and Activation Energy of the Different MnO_x Catalysts, with and without an External Reductant

Catalyst	$r_{nitroso}$ (10^{-10} mol/m^2 s)	$S_{nitroso}$ (%)	S_{BET} before (m^2/g)	S_{BET} after (m^2/g)	E_a (kJ/mol)
MnO(a)	29.2	100	2	2	144
With 300 mbar CO	31.7	72	2	2	32
Mn_3O_4(a)	5.5	92	13	13	110-130
With 150 mbar CH_4	6.0	84			
With 150 mbar CO	7.2	75		14	58
With 300 mbar CO	6.5	67			33
With 450 mbar CO	7.3	69			
With 600 mbar CO	7.2	68			
Pretreatment with H_2	9.1	55		15	
Mn_3O_4(b)	5.2	96	16	16	
Mn_3O_4(c)	7.3	99	4	4	139
With 300 mbar CO	14.2	87	4	3	103
Mn_3O_4(ox)	3.2	90	36	32	110
First 2 h at 623 K under He	2.5	88	36	29	112
First 24 h at 623 K under He	2.0	92	36	33	157
Mn_2O_3	6.6	92	15	8	108
MnO_2	5.0	100		5	

Note. See text for the definition of $S_{nitroso}$.

argon for 10 h at 573 K, the reduction to MnO takes place at a higher temperature, namely at 703 K. The small peak at 483 K disappears by Ar treatment. Reduction of the spent catalyst (after the reaction with nitrobenzene) takes place at a slightly higher temperature (723 K) than of the catalyst flushed with argon.

Fresh Mn_3O_4(c) is reduced at a slightly higher temperature than fresh Mn_3O_4(a), namely at 763 K. There is also a shoulder at 608 K. The O/Mn ratio at 300 K is equal to 1.37. The "nonstoichiometry" observed here is thus in good agreement with the data obtained by other techniques.

Catalytic Activity and Selectivity

The results of the catalytic experiments are, together with other relevant data, shown in Table 2 and in Figs. 3, 4, and 5. The catalysts of the initial composition MnO, Mn_2O_3 and MnO_2 change during the reaction with nitrobenzene as has been reported above. Although these catalysts will be coded as MnO, Mn_2O_3, and MnO_2, respectively, the reader has to keep in mind that this is not the steady state composition of the catalysts. Figure 2 shows the detected main and side products of the reaction of nitrobenzene. The rate of reaction and the selectivity for nitrosobenzene (for the definition see below) as shown in Table 2 were measured in the stage nearing the steady state of the reaction, after about 17 h (or longer) on stream.

The rate of reaction is defined as the nitrosobenzene concentration (detected by GC), times the gas flow, taken per unit surface area. The rate is then expressed in 10^{-10} mol/m^2 s. It is convenient to define a partial selectivity by a ratio of nitrosobenzene concentration divided by the sum of nitrosobenzene, aniline, and benzene concentrations.

The activation energy has been determined by the formal formula $\ln r = \ln A - E_a/RT$, where r is the rate of reaction, A is a constant, E_a is the apparent activation energy, R is the gas constant, and T is the temperature in degrees kelvin.

It must not be forgotten that nitrobenzene also disappears from the feed by reactions other than the selective reduction to nitrosobenzene (Fig. 2).

1. In the "autoredox" mode, i.e., a process without an external reductant, a certain amount of nitrobenzene is consumed to produce oxygen vacancies and CO, CO_2, and H_2O. A minimum of 7–14% of the nitrobenzene amount is used for such reduction to nitrosobenzene; if oxygen is removed in the form of higher alcohols or acids, this percentage is higher.

2. Condensation reactions to azobenzene, azoxyben-

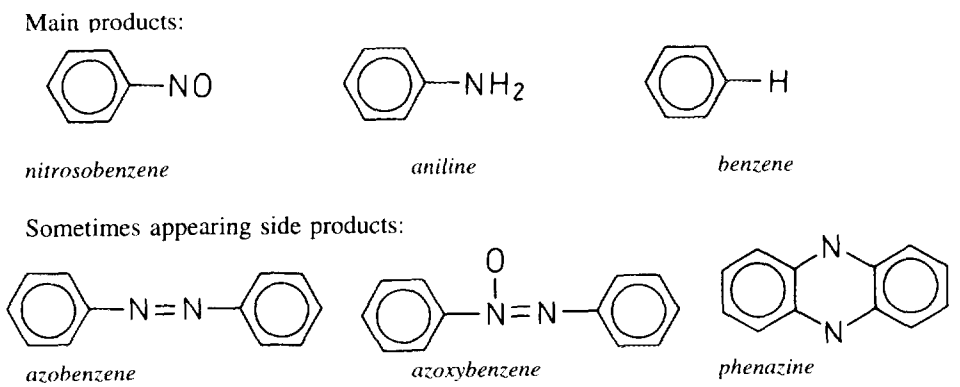

FIG. 2. The products of the reduction of nitrobenzene over manganese oxide. Benzene, when observed, is always present in small amounts.

zene, and phenazine also lead to a consumption of nitrobenzene.

3. Side reactions can lead to a low deposition of carbonaceous and hydrogen- and oxygen-lean layers.

4. An additional 1% of the amount of nitrobenzene that is used for the conversion to nitrosobenzene is converted into detected products with two to five carbon atoms.

None of the products just mentioned above could individually and quantitatively be determined "on line" by the equipment used. However, a rough estimate could be made of the total consumption of nitrobenzene by all reactions under 1 to 4 as follows. The concentration of nitrobenzene in the feed is compared with the nitrobenzene concentration at the output of the reactor and this difference is compared with the sum of concentrations of nitrosobenzene, benzene, and aniline. These measurements revealed that in the presence of an external reductant (CO) the losses of nitrobenzene to other products than benzene, aniline, and nitrosobenzene are in the limit of errors of the determination. In the "autoredox" mode, the situation is different. A rough estimate is that in some cases up to 50% of the reacted and lost nitrobenzene can take part in the above-mentioned reactions. If all carbon from the "lost" nitrobenzene just accumulated on the catalyst, three to five layers of carbonaceous species would be formed after about 17 h.

It can be seen from Table 2 that the areal rate of reaction with MnO is much higher than the rate with Mn_3O_4 as a catalyst. On the other hand, the rate of reaction with Mn_3O_4 is equal to the rate of reaction with the Mn_2O_3 and MnO_2 catalysts.

In the steady state of the reaction, these four catalysts do not show much difference in their selectivity patterns, and all are showing a high partial selectivity to nitrosobenzene (between 90 and 100%). As seen by UV/VIS spectroscopy applied to the condensates from the gas phase, Mn_3O_4 also forms in the autoredox mode small amounts of phenazine. MnO_2 shows a higher selectivity to oxidation and self-poisoning, indicating that the steady state has not yet been reached here. Also, more benzene is formed with the latter catalyst.

The rate of nitrosobenzene formation in the steady state is almost equal for Mn_3O_4(a) and Mn_3O_4(b), while the rate of reaction with Mn_3O_4(c) is slightly higher (Table 2). Figure 3a shows the course of the reaction with Mn_3O_4(a) as a catalyst. In the beginning of the reaction the nitrobenzene concentration decreases strongly, indicating adsorption on the surface and/or reduction of the catalyst. The latter reaction creates oxidation products such as CO and CO_2. At the same time, aniline is formed, showing a maximum concentration at about 3 h on stream. Then, the concentration of aniline decreases strongly. Formation of nitrosobenzene starts after about 1 hr on stream and it increases until a steady state has been reached.

Mn_3O_4 prepared from MnO_2 (Mn_3O_4(c)) does not show any formation of aniline and benzene in the steady state of the reaction.

Pretreatment of Mn_3O_4(a) with H_2 for 3 h at 650 K reduces the surface layers to MnO, as is indicated by the green colour of the oxide. This reduced catalyst shows a very different selectivity pattern in the course of the reaction in comparison with unreduced Mn_3O_4 (Fig. 3b). Here, immediately after adding nitrobenzene to the gas flow, the colour of the catalyst changes from green to brown, indicating oxidation of the surface layers. Moreover, in the beginning of the reaction only aniline is formed. In the steady state, the areal rate of nitrosobenzene formation is nearly two times higher than in the case of Mn_3O_4 without any pretreatment with H_2. However, the selectivity to aniline is much higher with the reduced catalyst: 45% instead of 8%.

XRD results show that the spent catalyst just discussed does not contain any MnO. This indicates that H_2 reduces only the surface layers of Mn_3O_4.

In another experiment, Mn_3O_4(a) was preoxidised (code Mn_3O_4(ox)). The X-ray diffraction pattern of the catalyst did not change by oxidation, which (as we mentioned

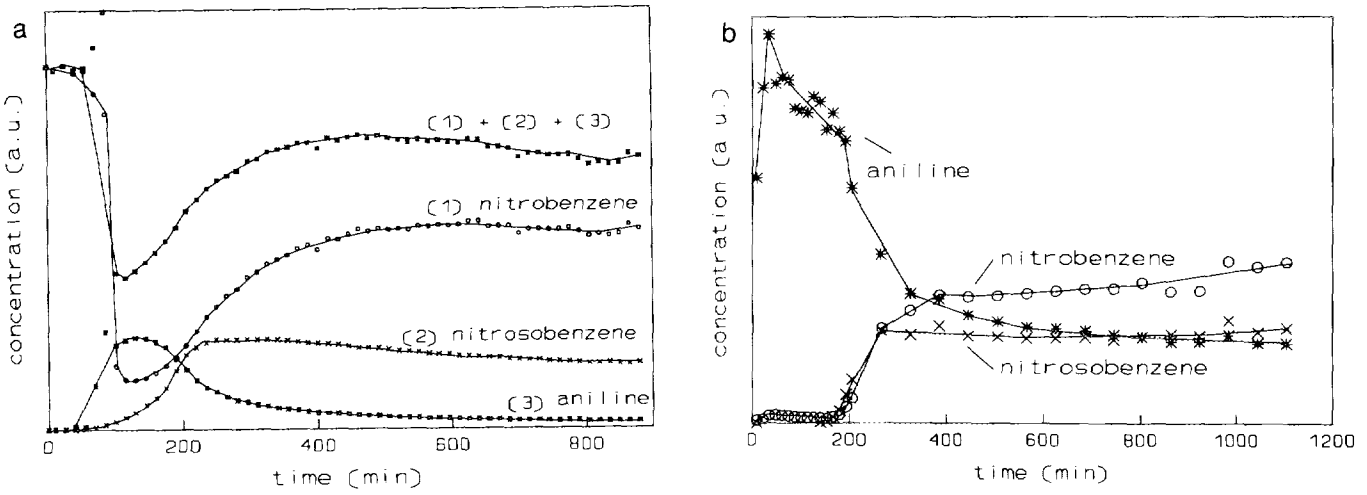

FIG. 3. (a) A typical time course of the reaction. The concentration of nitrosobenzene, aniline, nitrobenzene, and the sum of the former three, all as a function of time on stream, for the catalyst Mn_3O_4(a), under standard conditions and in autoredox mode. (b) The concentration of nitrobenzene, nitrosobenzene, and aniline as a function of time for Mn_3O_4(a), pretreated with H_2.

above) means that an increase of the average valency was not accompanied by a change in the crystallographic structure, or epitaxial Mn_2O_3 with a spinel structure has been formed, or only the surface layers consist of Mn_2O_3. However, the IR spectra and the colour of the catalyst indicate that oxygen was introduced into the lattice.

After an *ex situ* preoxidation, the Mn_3O_4(ox) catalyst was pretreated *in situ* in the following ways:

1. Mn_3O_4(ox) was immediately brought into contact with the reacting gas (nitrobenzene in helium, standard flows and concentrations).
2. Mn_3O_4(ox) was first flushed by helium for 2 h at 623 K.
3. The same procedure as under 2, for 24 h.

In all cases, the concentrations of nitrosobenzene and aniline change with time on stream in qualitatively the same way (similar to Fig. 3a). In all cases, aniline production starts almost immediately, as with the Mn_3O_4(a) catalyst. However, the formation of nitrosobenzene with Mn_3O_4(ox) starts only after about 6 h on stream, when no *in situ* pretreatment has been carried out (case 1). The production of nitrosobenzene sets in earlier when the flushing by helium has been prolonged. It is worthwhile mentioning that the originally dark-brown colour of Mn_3O_4(ox) changes into a lighter brown colour when the production of nitrosobenzene starts. This brown colour is, as mentioned above, typical for the Mn_3O_4 steady-state catalyst.

The observations made with the various manganese oxides can be summarised by the scheme in Fig. 4: whatever the initial form of the manganese oxide the steady-state composition of the surface layer is very near to that of Mn_3O_4. We have seen that this is indicated both by catalytic and by other, surface characterising, data (IR, UV/VIS, TPR).

With Mn_3O_4(a), the variation of the rate of reaction with the varying flow rate revealed that a higher flow rate increases the selectivity to nitrosobenzene and decreases the selectivity to aniline. This shows that a part of aniline is formed by a consecutive reaction via desorption and readsorption.

The Effect of an External Reductant (CH_4, CO)

All data presented above were obtained with a feed of nitrobenzene/helium. This means that no external reductant was present in the feed and oxygen atoms of the NO_2 group were converted into CO, CO_2, H_2O, etc., by fragments of the phenyl ring of nitrobenzene. However, it can be expected that the reaction rate and the selectivity would be influenced by the presence of an external reductant, which would compete for the same sites that adsorb and oxidise the phenyl ring (or its fragments). Moreover, the external reductant can possibly create additional oxygen vacancies which would then participate in the selective removal of oxygen from nitrobenzene.

Figure 5a shows the course of the reaction of Mn_3O_4(a) with methane (150 mbar) as the external reductant. In

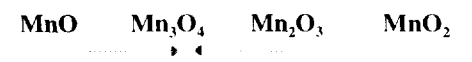

FIG. 4. Approach to the steady-state composition in the steady state of the reaction of the nitrobenzene reduction. Various manganese oxides have been used as catalysts in their initial form of the nominal composition as indicated.

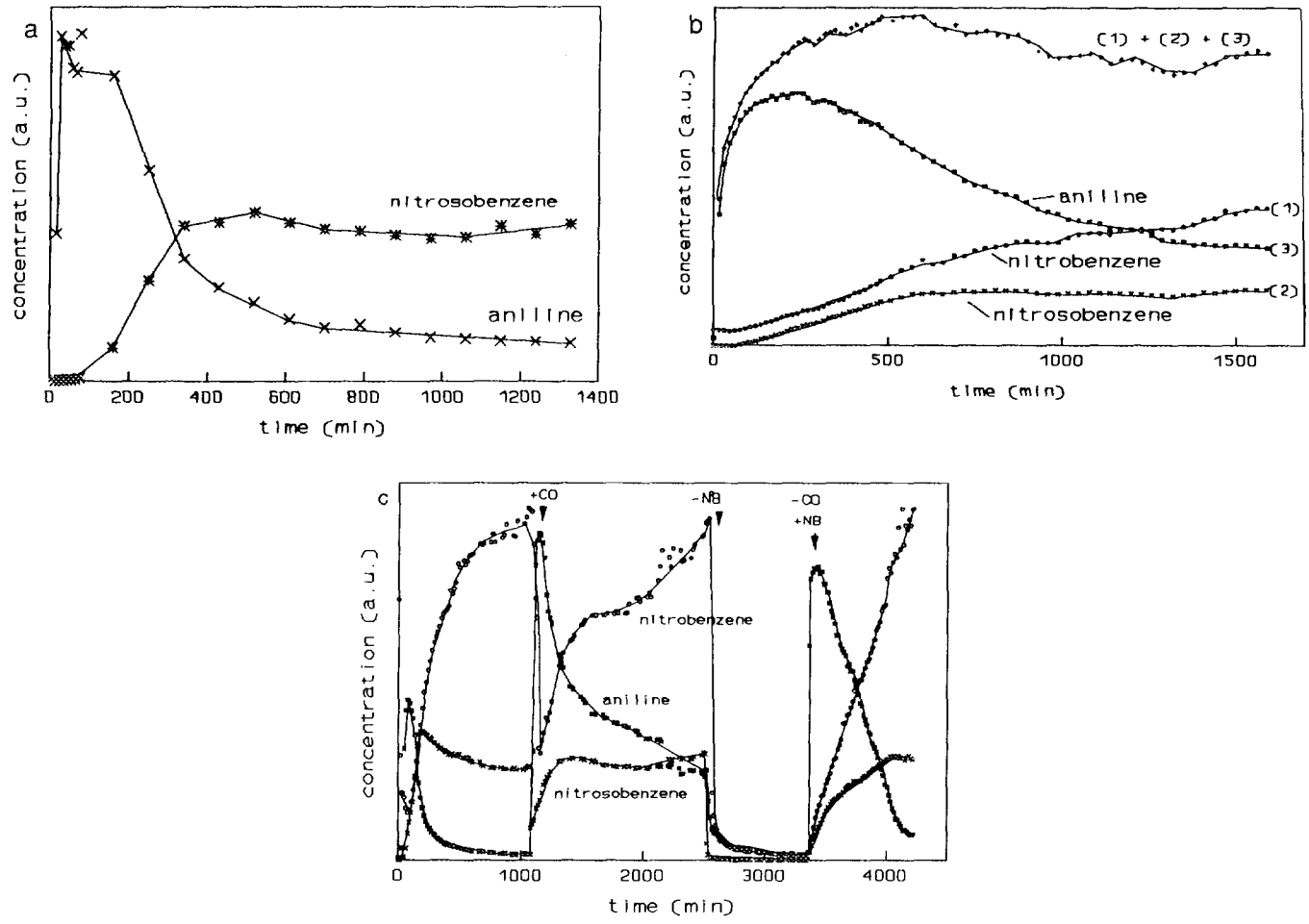

FIG. 5. (a) A typical time course of the reaction in a flow of gases. The concentration of nitrosobenzene and aniline as a function of time on stream, with methane as the external reductor. The catalyst is Mn_3O_4(a). (b) The concentration of nitrobenzene, nitrosobenzene, aniline, and the sum of the former three as a function of time, with CO as the external reductor. The catalyst is Mn_3O_4(a). (c) Product concentrations as a function of time on stream: influence of the presence (+) or absence (−) of CO and nitrobenzene (NB) in the feed, with the catalyst Mn_3O_4(a).

the initial state of the reaction, only aniline is formed. However, in the steady state of the reaction, the partial selectivity to nitrosobenzene is 84%. The reaction rate in the steady state does not seem to be much influenced by the presence of methane, a reductant recommended by the patent literature.

If CO is used as an external reductant, and Mn_3O_4 as a catalyst, the production of aniline (a loss of two instead of one oxygen atom per molecule) is higher than that in the absence of CO. As a consequence, the selectivity to nitrosobenzene is lower, being now only about 70%. The rate of nitrosobenzene formation does not change by addition of CO to the reaction mixture. There is no detectable formation of products with two to five carbon atoms and of benzene.

However, the formation of condensation products increases strongly when CO is used as an external reductant. Analysis of UV/VIS spectra revealed that the condensed products mainly consist of azobenzene, azoxybenzene, and phenazine. The apparent activation energy with Mn_3O_4(a) as a catalyst decreases from 120 kJ/mol to about 50 kJ/mol in the presence of CO in the feed.

The selectivity to aniline in the steady state of the reaction can be enhanced not only when CO is used as a continuously present reductant, but also when it is used for a reductive pretreatment of the catalyst (see Fig. 5b). In this experiment the catalyst was first pretreated with 300 mbar CO at 573 K for 16 h, whereby a part of the surface layers has been reduced up to MnO (green colour). After this CO pretreatment, the subsequent steady-state partial selectivity to nitrosobenzene is low, only 40%. However, the areal rate of reaction of nitrosobenzene formation is about two times higher with CO than with the same Mn_3O_4(a) without an external reductant. When the steady state was reached, CO was removed from the feed. There was an immediate increase in observable ani-

line production, followed by its sharp decrease. The rate of nitrosobenzene formation did not change. However, when CO was removed from the reaction mixture, the number of side reactions (see above) increased.

The role of CO as an external reductant has been checked in still another way (Fig. 5c). The autoredox reaction (nitrobenzene/helium mixture) was allowed to reach a steady state at 573 K. Then, CO was added to the reaction mixture. Immediately, the aniline production increased, while the nitrosobenzene production remained unchanged. When the steady state was reached again, the nitrobenzene was removed from the feed. Immediately, the production of nitrosobenzene ceased. However, the decrease in aniline production was much slower. This indicates that nitrosobenzene is not formed by oxidation of aniline. Subsequently, the catalyst was reduced by CO for 13 h at 573 K. Then, the CO flow was stopped and nitrobenzene was added to the feed again. The steady state of the reaction was about the same as that with Mn_3O_4(a) without the CO pretreatment. Only in the very initial state was the aniline production much higher with the pretreated catalysts.

We have seen that, with Mn_3O_4(a) as a catalyst, CO strongly increases the selectivity to aniline. However, Mn_3O_4(c), prepared from MnO_2, shows a selectivity pattern different from that of Mn_3O_4(a) when CO is introduced into the feed. Again, there is an increase in the rate of nitrosobenzene formation by a factor of two, but there is less reduction up to aniline. Furthermore, the apparent activation energy for Mn_3O_4(c) decreases when reduction is performed with CO, from 139 to 103 kJ/mol.

MnO shows a change in the selectivity pattern upon using an external reductor similar to that of Mn_3O_4(a). Again, there is an increase in the formation of aniline and condensation products. Furthermore, as with Mn_3O_4(a), the production of nitrosobenzene does not show a significant change when CO is added to the feed.

With or without CO, the colour of the catalyst always changes from green to brown after introduction of nitrobenzene; the presence of CO does not prevent the conversion of the surface layers of MnO into an oxide of a higher oxidation state. The apparent activation energy decreases strongly in this case, from 144 to 32 kJ/mol with the presence of CO in the feed.

DISCUSSION

Composition of the Oxides in the Working State of the Catalyst

All data show that Mn_3O_4 is always the stable phase, forming the surface of the steady-state catalysts in the selective reduction of nitrobenzene to nitrosobenzene, under our standard conditions. By the reaction, Mn_3O_{4+x} (as prepared) converts obviously into an Mn_3O_{4-y} oxide. According to Sadykov (11) *et al.*, the stationary form of MnO_x in the oxidation of CO is exactly the same for all manganese oxides, which is between Mn_3O_4 and Mn_3O_{4+x}. Thus, the CO oxidation tolerates superstoichiometric oxygen, while reduction of nitrobenzene does not.

Mn_2O_3 is more stable upon reaction with nitrobenzene than MnO_2. After 1 day of reaction on stream, only a small part of Mn_2O_3 is reduced to Mn_3O_4 and the UV/VIS spectra show that the surface of the catalyst is not deeply reduced. With the MnO catalyst one can think of a thick layer of Mn_3O_4 around the original manganese oxide. Such a model has been proposed earlier for Co_3O_4 (13).

The TPR experiments with Mn_3O_4(a) show that flushing the catalyst with argon decreases the reducibility, possibly because of sintering of the catalyst. The spent catalyst does not show much change in the TPR reduction temperature compared with the fresh catalyst that is flushed first with argon for 10 hr. This implies that the decrease of activity during the reaction cannot be explained by a decrease in the reducibility of the catalyst. The small peak at 483 K vanishes by argon flushing at 573 K and therefore can possibly be attributed to hydroxyl groups on the surface or to suprastoichiometric oxygen.

The shoulder at 608 K for Mn_3O_4(c) could indicate the presence of an additional phase, probably that of Mn_2O_3. The experiments described in (14) support this explanation. Together with the observation that the colour of the surface of Mn_3O_4(c) is brown, but darker than the colour of the surface of Mn_3O_4(a), it can be concluded that the oxide Mn_3O_4(c) contains more of the superstoichiometric oxygen than the Mn_3O_4(a) catalyst.

Catalytic Activity and Selectivity

Together with the existing information on the adsorption of reaction components (15), results obtained can lead to a suggestion on the detailed mechanism of the reaction. Before we formulate our suggestion, we shall present an inventory of relevant information on:

1. The adsorption modes of nitrobenzene
2. The possible mechanism
3. The state of the catalyst surface and its relation to the activity and selectivity in the nitrobenzene reduction.

Subsequently, we shall make an attempt to interrelate points 1 to 3.

1. The adsorption modes of nitrobenzene. Infrared spectra of nitrobenzene adsorbed on Mn_3O_4 (and Al_2O_3) (16) revealed that one adsorption mode is most likely a nitrobenzene molecule standing more or less perpendicularly on the surface (17, 18) (Fig. 6, mode A). However, it is a rather weak bond, leading to only modest shifts in the vibration frequencies ($\Delta\nu < 10$ cm^{-1}, with regard to

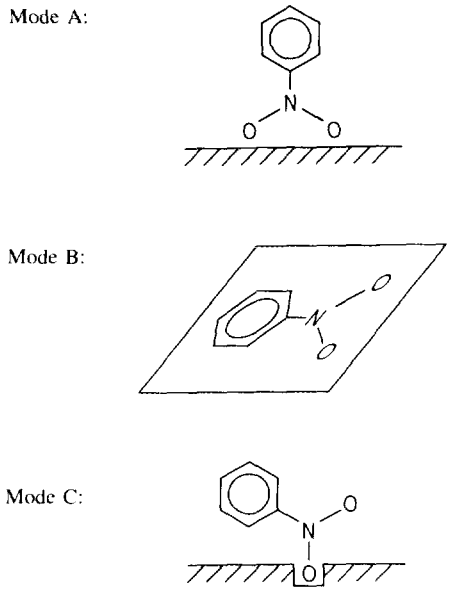

FIG. 6. Different adsorption modes of nitrobenzene on Mn_3O_4.

the liquid nitrobenzene). Tench *et al.* (19) deduced from the ESR spectra that nitrobenzene is adsorbed on MgO as a molecule laying flat on the surface (see Fig. 6, mode B).

The surface of MgO is rather flat and does not tolerate many defects like oxygen vacancies, and yet, when a hydrogen donor (e.g., methanol) is supplied, it can catalyse the reduction of nitrobenzene to aniline (20). Since with MgO the oxygen atoms of nitrobenzene probably do not find enough oxygen vacancies with which to react, and the bond Mg^{2+}–ONOPh is rather weak, while the reaction takes place at 620 K (20), the most likely orientation of nitrobenzene is flat on the MgO surface, as deduced from the ESR measurements.

Adsorption mode B (Fig. 6, mode B) is also predicted by the quantum chemical calculations on the electronic structure of nitrobenzene (21). According to (21) the positive charge is accumulated around the C–C bonds of the ring of nitrobenzene and this will be the place where the negatively charged O or OH of the oxide surface would attack the molecule. Aniline and benzene, on the other hand, have a negative charge around the C–C bonds of the ring. The flat-laying molecule (mode B) is thus the best candidate for being the intermediate of the oxidative destruction of the phenyl ring and of the creation of O vacancies in the catalyst surface. Another place of the positive charge is in the C–N region. Splitting of this bond produces benzene.

There should also be an adsorption mode (not yet identified by IR spectra or other spectra) which enables an easy removal of just one of the oxygen atoms of nitrobenzene. Such selective removal is not possible on MgO (also with hydrogen donors present) but almost all transition metal oxides can do it (22). Transition metal oxides distinguish themselves from MgO by varying valencies and, as a consequence, by easily tolerating defects such as oxygen vacancies, required for mode C (Fig. 6). The defects appear (by action of an external reductant or by the phenyl ring upon "autoreduction") here more abundantly and stationary, at such temperatures where the reaction of dissociation of one N–O bond and the reoxidation of the surface are fast. The distribution of charges in the nitrobenzene favours this adsorption mode (21).

By dissociation, nitrosobenzene is created, which, however, has a different charge distribution than nitrobenzene: the C–N region is now slightly negative, which stimulates nitrosobenzene desorption. This is likely the reason why no strong adsorption of nitrosobenzene could ever be detected by the IR spectra (15). An orientation, such as that in mode C in Fig. 6, is known in the coordination chemistry of nitroarenes (23). It enables the operation of the Mars and Van Krevelen mechanism.

2. The possible mechanism. Essentially, there are two different mechanisms of the selective oxidation/reduction reactions at medium temperatures:

a. The Mars and Van Krevelen mechanism (MVKM) by which oxygen of the oxide lattice appears in the oxidation products and oxygen of a molecule to be reduced is delivered to the lattice.

b. The Langmuir–Hinshelwood mechanism (LHM) taking place in the adsorbed layer without any participation of the lattice components.

There is abundant evidence (24) that the selective oxidation of most of the interesting organic molecules takes the form of a two-step process (MVKM), whereby the lattice vacancy is replenished by oxygen from dioxygen in the reaction mixture.

It is likely (see under 1) that with oxides, which do not bear a sufficient concentration of oxygen vacancies like MgO, the reduction, e.g., by methanol, happens by the Langmuir–Hinshelwood mechanism. With oxides, which easily lose or accept oxygen atoms, the situation is different. It has been established recently in our laboratory (25) that oxidation of nitrosobenzene (the reverse step of nitrobenzene reduction) takes place at substantially lower temperatures than the nitrobenzene reduction and can proceed by both principal mechanisms. On Mn_3O_4, the main part of the oxidation occurs by the lattice oxygen (MVKM). On Fe_2O_3 or MgO, most of the oxidation occurs by redistribution of oxygen amongst the adsorbed molecules (LHM). As we shall see below (under 3), everything that increases the number of oxygen vacancies increases also the rate of nitrosobenzene formation (and also the rate of aniline formation). Thus, we conclude that with the Mn_3O_4 catalysts the main part of nitrosobenzene is formed by the Mars and Van Krevelen mechanism.

3. The state of the catalyst surface and its relation to the activity and selectivity in the nitrobenzene reduction. We have seen above that whatever the initial state of the catalysts (from MnO to MnO_2), the steady state is near Mn_3O_4 (most likely, $MnO_{1.33-y}$). When we start with Mn_3O_4, the surface must first be reduced and oxygen vacancies created (nitrobenzene is consumed; see the first dip in Fig. 3a) before any nitrosobenzene appears. When we start with a slightly prereduced (by H_2 or CO) Mn_3O_4 or with MnO, the surface must be first reoxidised (Figs. 3b and 5b) before nitrosobenzene is produced in a stationary way. In these cases, the aniline production starts already in the very initial stages of the reduction. Nitrosobenzene is never observed with oxygen-rich surfaces (between Mn_2O_3 and MnO_2). Aniline production and the production of the condensation products (azobenzene, azoxybenzene, phenazine) are promoted by prereduction, i.e., by a higher average Mn^{2+}/Mn^{3+} ratio in the catalyst. The nitrosobenzene formation is thus related to a certain Mn^{2+}/Mn^{3+} ratio, i.e., to a certain concentration of oxygen vacancies.

Presence of a strong reductant, such as CO, prevents oxidation of the phenyl ring. However, it stimulates the production of easily condensing products of condensation reactions (such as phenazine, azobenzene, and azoxybenzene).

Let us now make an attempt to put all of this information into a consistent picture. When the surface of the manganese oxide must be reduced to achieve the steady state of the surface, adsorption mode B (Fig. 6) or an external reductant work well. When the surface must be extensively oxidised (as with MnO in the initial state), both modes A and B can in principle be the intermediates. The selective nitrosobenzene production seems to be related to a certain and limited range of composition (Mn^{2+}/Mn^{3+} ratio), and mode C seems to be a good intermediate for this reaction.

It is known from the literature that, for example, $Fe_3H(CO)_{11}$ or $Co_2(CO)_8$ adsorbed on Al_2O_3 can reduce nitroarenes into amines (26, 27). In homogeneous reductions, azo compounds are formed (28). Thus, all these reactions should also be possible by the Langmuir–Hinshelwood mode, without any participation of the lattice oxygen or oxygen vacancies (MVKM).

The steady-state aniline production seems to have a relation to the initial state of the catalyst, also in an aspect other than the initial Mn^{2+}/Mn^{3+} ratio. The catalysts prepared from a hydroxide have a higher steady state of aniline formation upon the autoreduction than the catalysts prepared by reduction MnO_2. The latter likely have less hydroxyl groups on their surface. Thus a more abundant presence of OH groups at the surface of the catalyst in its initial state stimulates the presence of OH groups in the steady state.

From what was said just above, aniline can be produced not by one but by a variety of reactions:

a. by a consecutive reaction, from nitrosobenzene (probably a small steady-state contribution).

b. by a multiple dissociation of N–O bonds (adsorption of nitrobenzene, modes A and B, Mars and Van Krevelen mechanism),

c. by a reaction in the adsorbed layer (Langmuir–Hinshelwood mechanism), with H or OH as potential reductors (CO does not react in this way) (25)).

On the other hand, the rate of the nitrosobenzene production is not influenced by switching the CO cofeed "off" or "on." Therefore, we suggest that nitrosobenzene cannot be produced by a Langmuir–Hinshelwood-type reduction, but is exclusively produced by the Mars and Van Krevelen mechanism, starting from an intermediate like mode C (Fig. 6). The effect of CO is stronger at low temperatures when the reduction of the surface by the phenyl ring is slow. This leads to an apparent decrease of the activation energy of the nitrosobenzene production, as shown in Table 2.

CONCLUSIONS

1. At variance with the patent literature, MnO_2 is found to be a good precursor of a steady-state catalyst.
2. A well-defined valence state of the catalyst is established at the steady state.
3. The steady state is that of a slightly reduced spinel, Mn_3O_{4-y}. This contrasts with the steady states of spinels in the CO oxidation (Mn_3O_{4+x}).
4. A consistent picture relating the valency state, adsorption modes, activity, and selectivity of the catalyst can be suggested.

ACKNOWLEDGMENTS

The authors thank A. Andreini from the University of Amsterdam for performing the TPR experiments and Dr. Rommers from Philips Laboratories for the chemical analyses. They also express their thanks to Professor J. Ziolkowski from the University of Krakow for valuable discussions. Financial support by NWO and Leiden University has been highly appreciated.

REFERENCES

1. Mars, P., and Van Krevelen, D. W., *Chem. Eng. Sci.* **3**, 41 (1954).
2. Dodman, D., Pearson, K. W., and Woolley, J. M., *Brit. Appl.* 1,322,531 (1973).
3. Zengel H. G., and Bergfeld, M., *Ger. Offen.* 2,939,692 (1981).
4. Favre, T. L. F., Maltha, A., Kooyman, P. J., Zuur, A. P., and Ponec, V., "Proceedings, XI Symposium Iberoam. Catal.," Guanajuato, Vol. 2, p. 807, 1988.
5. Boreskov, G. K., "Proceedings, 8th International Congress on Catalysis, Berlin, 1984." Dechema, Frankfurt-am-Main, 1984.

6. Bricker, O., *Am. Mineral.* **50,** 1296 (1966).
7. Potter, R. M. and Rossman, G. R., *Am. Mineral.* **64,** 1199 (1979).
8. Ishii, M., Nakahira, M. and Yamanaka, T., *Solid State Commun.* **11,** 209 (1972).
9. Ziolkowski, J., *Surf. Sci.* **209,** 536 (1989).
10. Ziolkowski, J., private communication.
11. Sadykov, V. A., Tsyrul'nikov, P. G., Popovskii, V. V., and Tikhov, S. F., *Kinet. Katal.* **22,** 951 (1981).
12. Jarosch, D., *Mineral. Petrol.* **37,** 15 (1987).
13. Petrov, L., Kumbilieva, K., and Kirkov, N., *Appl. Catal.* **59,** 31 (1990).
14. Yang, Y., Huang, R., Chen, L., and Zhang, J., *Appl. Catal. A,* **101,** 233 (1993).
15. Koutstaal, C. A., Angevaare, P. A. J. M., and Ponec, V., accepted for publication.
16. Koutstaal, C. A., Angevaare, P. A. J. M., Grootendorst, E. J., and Ponec, V., *J. Catal.* **141,** 82 (1993).
17. Cenini, S., Pizzotti, M., and Crotti, C., *in* "Aspects of Homogeneous Catalysis," Vol. 6, p. 97. Reidel, Dordrecht, 1988.
18. Driessen, W. L., van Geldrop, L. M., and Groeneveld, W. L., *Recl. Trav. Chim. Pays Bas* **89,** 1271 (1970).
19. Tench, A. J., and Nelson, R. L., *Trans. Faraday Soc.* **63,** 2254 (1967).
20. Kijenski, J., Glinski, M., Wisniewski, R., and Murghani, S., *Stud. Surf. Sci. Catal.* **59,** 169 (1991).
21. Politzer, P., Abrahmsen, L., and Sjoberg, P., *J. Am. Chem. Soc.* **106,** 855 (1984).
22. Maltha, A., van Wermeskerken, S. C., Favre, T. L. F., Angevaare, P. A. J. M., Grootendorst, E. J., Koutstaal, C. A., Zuur, A. P., and Ponec, V., *Catal. Today* **10,** 387 (1991).
23. Izakovich, E. N., and Khidekel, M. L., *Russ. Chem. Rev.* **57,** 419 (1988).
24. Golodets, G. I., *Stud. Surf. Sci. Catal.* **55,** 693 (1990).
25. Grootendorst, E. J., Leiden University, private communication.
26. Alper, H., and Gopal, M., *J. Chem. Soc. Chem. Commun.* 821 (1980).
27. Alper, H., and Gopal, M., *J. Organomet. Chem.* **219,** 125 (1981).
28. Alper, H., and Paik, H., *J. Organomet. Chem.* **144,** C18 (1978).